Springer

Journal of
Mechanical
Science and
Technology

Journal of Mechanical Science and Technology 23 (2009) 1602~1612

www.springerlink.com/content/1738-494x
DOI 10.1007/s12206-009-0427-z

Analysis of the combustion instability of a model gas turbine combustor by the transfer matrix method †

Dong Jin Cha[1,*], Jay H. Kim[2] and Yong Jin Joo[3]

[1]*Department of Building Services Engineering, Hanbat National University, Daejeon, 305-719, Korea*
[2]*Department of Mechanical Engineering, The University of Cincinnati, Cincinnati, Ohio, 45221 U.S.A.*
[3]*IGCC Group, Korea Electric Power Research Institute, Daejeon, 305-380, Korea*

(Manuscript Received December 9, 2008; Revised April 1, 2009; Accepted April 12, 2009)

Abstract

Combustion instability is a major issue in design of gas turbine combustors for efficient operation with low emissions. A transfer matrix-based approach is developed in this work for the stability analysis of gas turbine combustors. By viewing the combustor cavity as a one-dimensional acoustic system with a side branch, the heat source located inside the cavity can be described as the input to the system. The combustion process is modeled as a closed-loop feedback system, which enables utilization of well-established classic control theories for the stability analysis. Due to the inherent advantage of the transfer matrix method and control system representation, modeling and analysis of the system becomes a straightforward task even for a combustor of the complex geometry. The approach is applied to the stability analysis of a simple combustion system to demonstrate its validity and effectiveness.

Keywords: Combustion instability; Model gas turbine combustor; Normal mode method; Stability margin; Thermoacoustics; Transfer matrix method

1. Introduction

Combustion instability is induced by the coupling effect of the unsteady heat release of the combustion process and the change in the acoustic pressure in the gas manifold of the combustion chamber [1-4]. Such instabilities can cause various problems in the combustion system such as poor efficiency, premature degradation of components, and even a catastrophic failure of the system. Because of the complexity and nonlinearity involved in the phenomenon, an accurate, full-scale quantitative analysis is very difficult. However, a simple and reliable analysis method based on a linear model can be developed to understand the condition of the instability and obtain design guidelines.

The main motivation of this paper was to develop a new approach based on the transfer matrix method to model combustion systems. The transfer matrix, which is also called four-pole matrix, is a very convenient concept to model a complex acoustic system [5-7]. The method has been primarily used for one-dimensional systems, but can also be applied to three-dimensional systems with proper modifications [8]. Richards et al. applied the transfer matrix method to model the combustion system as a feed-back control system [4]. In their model, the transfer matrix method was applied to calculate impedances at various points, which were used to assemble the system model.

In the method we developed, the combustion system is modeled by using a duct system with a side branch to represent the flame point as the system input. Combined with the transfer matrix method, this approach enables much simpler and straightforward modeling of the combustor system.

The transfer matrix method and the new approach provide the following advantages.

† This paper was recommended for publication in revised form by Associate Editor Ohchae Kwon

* Corresponding author. Tel.: +82 42 821 1182, Fax.: +82 42 821 1175
E-mail address: djcha@hanbat.ac.kr

- Modeling of a combustion system composed of multiple sections is as straightforward as modeling a system with a single section cavity.
- Spatial change of the temperature in the combustion system can be easily handled by dividing the system into multiple sections.
- Analysis of the effect of passive control devices can be readily incorporated.

In addition, the control system representation of the model enables the following advantages.

- Well-established classic control analysis methods such as the root-locus method and Nyquist plot can be applied directly.
- The stability margin can be obtained, which can be very useful design information.

2. Description of the system by a wave Eqn.

Fig. 1 shows a simple combustion system. A large plenum is attached to the left end, which is modeled as the pressure release end. The flow is restricted at the right end, which is modeled as the close end. The heat source at $x = b$ is represented as a point source. The combustion process is described by the following non-homogeneous acoustic wave equation [9].

$$\frac{1}{c^2}\frac{\partial^2 p}{\partial t^2} - \nabla^2 p = h_w \tag{1}$$

where, p is the acoustic pressure, c is the speed of sound and h_w is the source term due to the combustion. For the 1-D system shown in Fig. 1, the equation becomes [3]

$$\frac{1}{c^2}\frac{\partial^2 p}{\partial t^2} - \frac{\partial^2 p}{\partial x^2} = \frac{\gamma - 1}{c^2}\frac{\partial q}{\partial t}\delta(x-b). \tag{2}$$

Where, q is the rate of heat release per area and $\delta(x-b)$ is the Dirac delta function. Various models are used to relate the heat release and acoustic variables. One of simple models [3] is

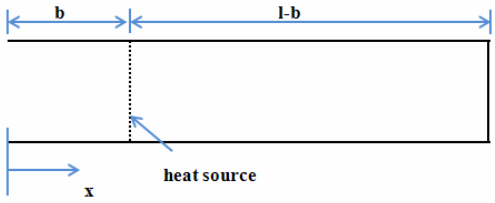

Fig. 1. A simple combustion system.

$$q(t) = -\frac{\beta\rho c^2}{\gamma - 1}u(b^-, t-\tau). \tag{3}$$

Where, $u(b^-, t-\tau)$ is the particle velocity right before the flame, at $x = b^-$, τ is the time delay, which is related to the convection time from fuel injection to its combustion, and β is a non-dimensional parameter that has to be determined empirically.

Eq. (2) can be compared with the Lighthill's equation of the sound field, with a mass flow source [10].

$$\frac{1}{c^2}\frac{\partial^2 p}{\partial t^2} - \frac{\partial^2 p}{\partial x^2} = \frac{\partial(\dot{m})}{\partial t} \tag{4}$$

where, $\dot{m}$ is the mass flow input to the system per unit volume. By comparing Eq. (4) with Eq. (2), it is seen that

$$\frac{\gamma - 1}{c^2}Q(t) = \dot{m}(t) = \rho u_s = \rho\left(u(b^+, t) - u(b^-, t)\right). \tag{5}$$

Substituting Eq. (3) into Eq. (5) and simplifying, we find that

$$u(b^+, t) - u(b^-, t) = -\beta u(b^-, t-\tau). \tag{6}$$

If the flow is harmonic, etc, Eq. (6) becomes

$$U(b^+) = U(b^-)(1 - \beta e^{-j\omega\tau}). \tag{7}$$

Where, upper cases imply the harmonic amplitudes.

3. Review of two existing solution methods

3.1 Method based on assumed mode shape [3]

In the system shown in Fig. 1, the boundary conditions are

$$P(0) = 0,\ U(l) = 0. \tag{8}$$

The form of the solution that satisfies Eq. (8) is, in the domain $x < b$,

$$P(x) = A\sin(kx) \tag{9}$$

$$U(x) = \frac{j}{\rho c}A\cos(kx). \tag{10}$$

And in the domain $x > b$,

$$P(x) = B\cos[k(l-x)] \tag{11}$$

$$U(x) = \frac{j}{\rho c} B \sin[k(l-x)]. \tag{12}$$

At $x = b$, the pressure continuity condition is

$$A \sin(kb) = B \cos[k(l-b)]. \tag{13}$$

The velocity jump condition is

$$B \sin[k(l-b)] = 1 - \beta e^{-j\omega\tau}. \tag{14}$$

Combining Eqs. (13) and (14), the frequency equation is obtained as

$$\tan(kb)\tan[k(l-b)] = 1 - \beta e^{-j\omega\tau}. \tag{15}$$

The resonance frequency can be obtained by solving Eq. (15) by a numerical method. If the i^{th} root of Eq. (15) is ω_i, the normalized frequency and normalized growth rate [3] are obtained as

$$f_{N_i} = \frac{\mathrm{Re}(\omega_i)}{\omega_{ni}} \tag{16}$$

$$g_{N_i} = \frac{-\mathrm{Im}(\omega_i)}{\omega_{ni}} \tag{17}$$

where ω_{ni} is the i^{th} undamped resonance frequency. A positive growth rate g_{Ni} indicates that the combustion process will be unstable.

Fig. 2 shows the trend of instability as a function of the growth rate β and the time delay τ. The combustion process becomes unstable in the frequency range in that g_N is positive, and the magnitude of g_N indicates the strength of instability.

3.2 Solution by galerkin's method [2]

The pressure in the system can be assumed as a linear combination of the natural modes as follows.

$$p(x,t) = \sum_{m=1}^{\infty} \eta_m(t) \psi_m(x) \tag{18}$$

where, $\psi_m(x)$ is the m^{th} mode and η_m is the participation factor of the mode. Substituting Eq. (18) into Eq. (2) and applying the orthogonal property of the natural modes, we obtain

$$\frac{d_2\eta_m}{dt^2} + \omega_m^2 \eta_m = \frac{\gamma - 1}{\int_0^l \psi_m^2 dx} \int_0^l \frac{\partial q}{\partial t} \psi_m(x) dx. \tag{19}$$

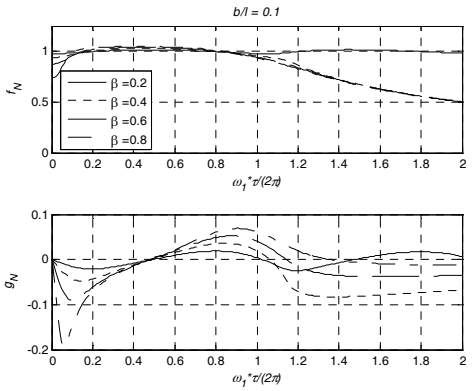

Fig. 2. Variation of instability frequency and growth rate with τ for the root of Eq. (15) near ω_{ni}, taking $b/\ell = 0.1$ and different βs (Similar to one in Ref. 3).

In the above, *m=1,2,3,…* It is seen that Eq. (19) is still coupled because

$$q(x,t) = Q(t)\delta(x-b) = -\frac{\beta\rho c^2}{\gamma - 1} u(b^-, t-\tau)\delta(x-b) \tag{20-a}$$

and, u in Eq. (20-a) is

$$\rho \frac{\partial u}{\partial t} = -\frac{\partial p}{\partial x} = -\frac{\partial}{\partial x} \sum_{m=1}^{\infty} \eta_m(t) \psi_m(x)$$

$$= -\sum_{m=1}^{\infty} \eta_m(t) \psi_m(x)'. \tag{20-b}$$

It was suggested to simply Eq. (19) by keeping only the fundamental mode ($m = 1$) in evaluating Eq. (20-a) [2]. Fig. 3 shows η_1 and $d\eta_1/dt$ obtained by the approach for several different values of τ when β is fixed at *0.2*. Fig. 3(a), the case when $\tau=0$, shows the disturbance remains constant. In Figs. 3(b) and (d), where g_N is negative, the disturbance decays. In Figs. 3(c), (e), and (f), where g_N is positive, the disturbance grows. In the latter case the disturbance grows the most slowly. These observations match with what we observed in Fig. 2.

4. Development of transfer matrix based methods

The transfer matrix method, also known as the four-pole method, is a powerful technique to analyze a built-up acoustic system [5-7]. The method is ideal for analyzing a combustor system composed of multiple sections of different cross-sections and side-branches [11]. Richards et al. used the method to obtain the system eqn. of a combustion manifold,

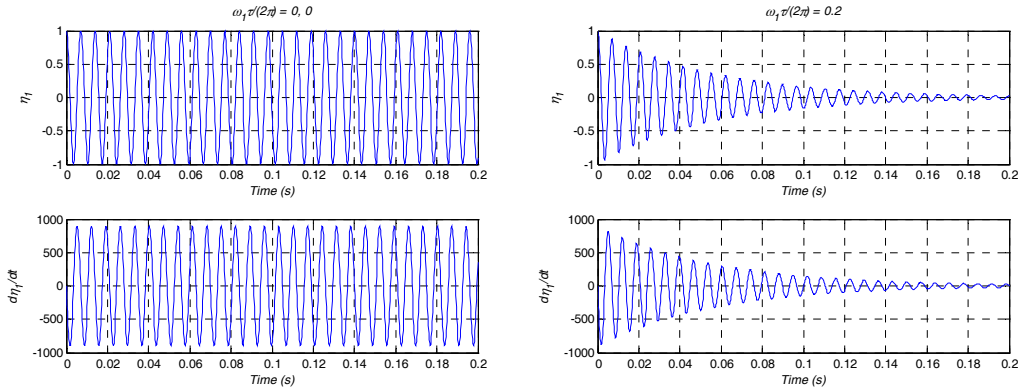

(a) $\omega_1\tau/(2\pi)$=0.0 (b) $\omega_1\tau/(2\pi)$=0.2

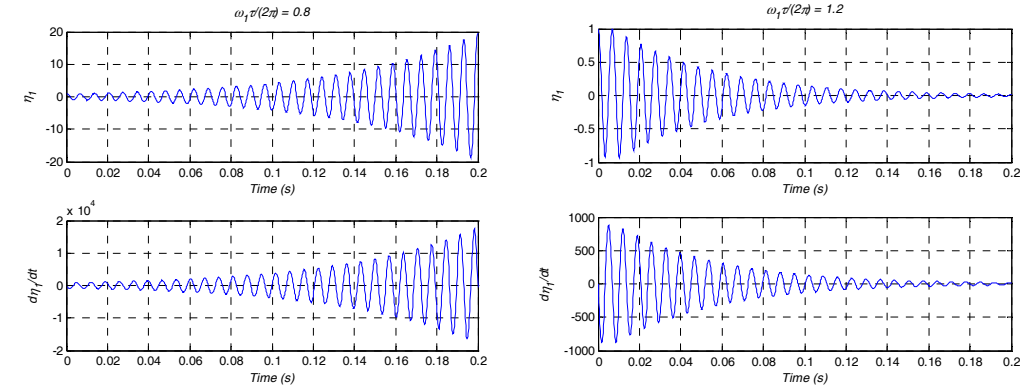

(c) $\omega_i\tau/(2\pi)$=0.8 (d) $\omega_1\tau/(2\pi)$=1.2

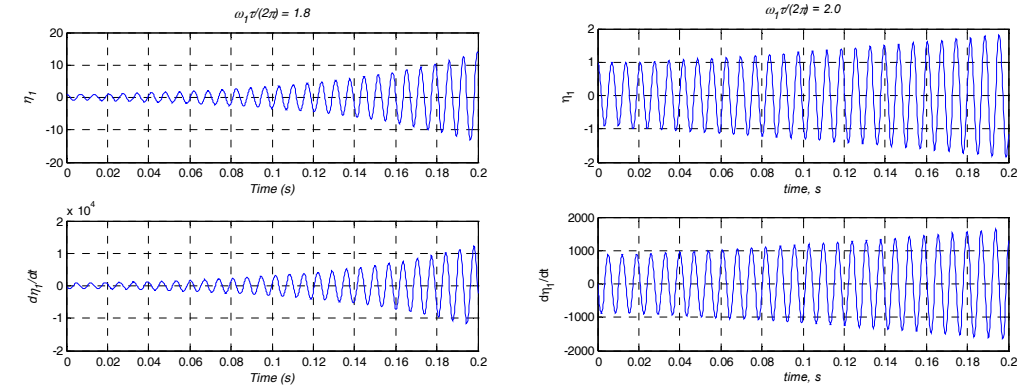

(e) $\omega_1\tau/(2\pi)$=1.8 (f) $\omega_1\tau/(2\pi)$=2.0

Fig. 3. Variation of disturbance in combustion dynamic pressure with β of 0.2 and different values of $\omega_1\tau/(2\pi)$ shown in Fig. 2.

which was then converted to a control system description of the model [4].

In this work, we developed a new approach to apply the transfer matrix method more easily for modeling the combustion system. The approach rearranges the system model to describe the heat source point as the input point of the system by viewing a part of the combustion duct as a side-branch. It is shown that the method is equivalent to the two methods we discussed previously.

Fig. 4 shows the 1-D system in Fig. 1 represented as a combination of two sub-elements. Fig. 4(a)

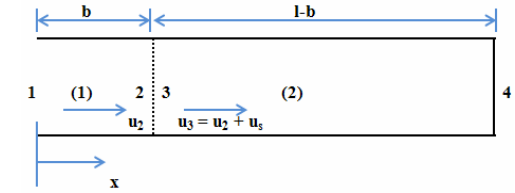

(a)

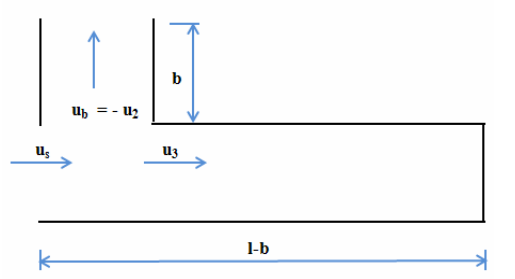

(b)

Fig. 4. Combustor modeled as a 1-D duct, (a) 1-D duct model, (b) 1-D duct model with a side branch description.

shows a typical model and Fig. 4(b) shows the system with the left end of the duct described as a side branch. The model in Fig. 4(b) enables the volume flow input u_s due to the heat release to be described as the system input. In the system shown in Fig. 4(a), the boundary conditions are given as

$$p_1 = 0,\ u_4 = 0. \tag{21}$$

It is more convenient to use acoustic mass flow velocity than the particle velocity in formulation of the transfer matrix because the cross-sectional area and temperature change throughout the system. For the i^{th} section of the duct, we define

$$V_i = \rho_i S_i U_i \tag{22}$$

where, V_i and U_i are harmonic amplitudes of the mass flow velocity and the particle velocity, ρ_i and S_i are the density and cross-sectional area of the i^{th} section of the duct. The transfer matrix of a duct of length L is given as [5]

$$\begin{bmatrix} A & B \\ C & D \end{bmatrix} = \begin{bmatrix} \cos(kL) & \frac{jc}{S}\sin(kL) \\ \frac{jS}{c}\sin(kL) & \cos(kL) \end{bmatrix}. \tag{23}$$

The system equation in the transfer matrix equation is given for the system shown in Fig. 4(b) as follows [8].

$$\begin{Bmatrix} P_2 \\ V_S \end{Bmatrix} = \begin{bmatrix} 1 & 0 \\ \frac{1}{Z_S} & 1 \end{bmatrix} \begin{bmatrix} A_2 & B_2 \\ C_2 & D_2 \end{bmatrix} \begin{Bmatrix} P_4 \\ U_4 \end{Bmatrix} = \begin{bmatrix} A_2 & B_2 \\ \frac{A_2}{Z_S} + C_2 & \frac{B_2}{Z_S} + D_2 \end{bmatrix} \begin{Bmatrix} P_4 \\ V_4 (= 0) \end{Bmatrix} \tag{24}$$

where, A_2, B_2, C_2 and D_2 are the four-pole parameters of the duct (2) of length *l-b* in Fig. 4 (a) and Z_s is the impedance of the side branch defined as

$$Z_S = \frac{P_b (= P_2)}{V_b}. \tag{25}$$

From Eq. (24),

$$P_2 = A_2 P_4 \tag{26}$$

and

$$V_S = \left(\frac{A_2}{Z_S} + C_2 \right) P_4. \tag{27}$$

Therefore,

$$P_2 = \frac{A_2}{\left(\frac{A_2}{Z_S} + C_2 \right)} V_S = P_b = Z_S V_b = Z_S (-V_2). \tag{28}$$

Also,

$$Z_S = \frac{P_b}{V_b}$$

$$V_2 = \frac{A_2}{Z_S \left(\frac{A_2}{Z_S} + C_2 \right)} V_S = -\frac{A_2}{A_2 + C_2 Z_S} V_S. \tag{29a}$$

In terms of particle velocities,

$$U_2 = -\frac{A_2}{A_2 + C_2 Z_S} U_S. \tag{29b}$$

Because $U_s = \frac{\gamma - 1}{\rho c^2} Q$ (see Eq. (5)),

$$Q = -\frac{\beta \rho c^2}{\gamma - 1} e^{-j\omega\tau} U_2 \tag{30}$$

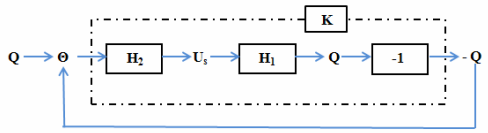

Fig. 5. Feedback loop description of the combustion process.

$$= -\frac{\beta\rho c^2}{\gamma-1} e^{-j\omega\tau} \frac{A_2}{A_2 + C_2 Z_S} U_S = H_1 U_S.$$

Where $H_1 = \frac{\beta\rho c^2}{\gamma-1} e^{-j\omega\tau} \frac{A_2}{A_2 + C_2 Z_s}$ is the transfer function between U_s and Q. The transfer function H_2 between Q and U_s is,

$$H_2 = \frac{U_S}{Q} = \frac{\gamma-1}{\rho c^2}. \tag{31}$$

Fig. 5 shows the combustion system described as a feedback loop. Notice that *-1* is multiplied to Q to make a negative feedback loop to adopt the standard convention adopted in control theory. From the figure, the open loop transfer function K is obtained as

$$\begin{aligned} K &= -H_1 H_2 \\ &= \frac{\beta\rho c^2}{\gamma-1} e^{-j\omega\tau} \frac{A_2}{A_2 + C_2 Z_S} \frac{\gamma-1}{\rho c^2} \end{aligned} \tag{32}$$

The closed-loop transfer function of the system is $\frac{K}{1+K}$ and the closed loop pole is found from the condition $K = -1$. This gives

$$\frac{\beta\rho c^2}{\gamma-1} e^{-j\omega\tau} \frac{A_2}{A_2 + C_2 Z_S} \frac{\gamma-1}{\rho c^2} = 1. \tag{33}$$

The side branch input point impedance is $Z_S = \frac{P_b}{V_b}$ found from the four pole equation between the input and output points of the side branch, which is

$$\begin{Bmatrix} P_b \\ V_b \end{Bmatrix} = \begin{bmatrix} \cos(kb) & \frac{jc}{S}\sin(kb) \\ \frac{jS}{c}\sin(kb) & \cos(kb) \end{bmatrix} \begin{Bmatrix} P_{be} = 0 \\ V_{be} \end{Bmatrix}. \tag{34}$$

Therefore, $Z_S = \frac{P_b}{V_b} = \frac{jc}{S}\tan(kb)$. Also with $A_2 = \cos[k(l-b)]$, $C_2 = \frac{jS}{c}\sin[k(l-b)]$, Eq. (33) becomes

$$\begin{aligned} &\frac{\beta\rho c^2}{\gamma-1} e^{-j\omega\tau} \times \\ &\frac{\cos[k(l-b)]}{\cos[k(l-b)] + \frac{jS}{c}\sin[k(l-b)]\frac{jc}{S}\tan(kb)} \times \\ &\frac{\gamma-1}{\rho c^2} = 1. \end{aligned} \tag{35}$$

Simplifying Eq. (35), we obtain the same characteristic equation Eq. (15) [3]. The open loop transfer function K, Eq. (35) is obtained as follows:

$$K = \frac{\beta}{1 - \tan[k(l-b)]\tan(kb)} e^{-j\omega\tau}. \tag{36}$$

5. Case study results and discussions

If the system in Fig. 1 has different temperatures in the sections before and after the heat source, the characteristic equation Eq. (15) becomes,

$$\tan[k_3(l-b)]\tan(k_2 b) = \frac{\rho_3 c_3}{\rho_2 c_2}(1 - \beta e^{-j\omega\tau}). \tag{37}$$

Also, the open loop transfer function Eq. (36) becomes,

$$K = \frac{\beta}{1 - \tan[k_3(l-b)]\tan(k_2 b)} e^{-j\omega\tau}. \tag{38}$$

In general, a gas turbine combustion system can be modeled as a network of fuel injector including air and fuel supplies, flame, combustion chamber, exhaust nozzle, etc. [4, 12]. Table 1 lists the parameters used for the simulations. All parameters in the table, both geometrical and operational, are selected from representative values of gas turbine combustors.

Fig. 6 shows the simulation result. The Fig. shows that the oscillation grows or decays depending on the input β and the time delay τ. For τ =0 (not reported here) the rate of heat input only shifts the frequency of the oscillation.

Table 2 summarizes the simulation results for β = *0.2* shown in Fig. 6. The data in the first column is the first transition point of the mode from the stable to unstable conditions. For example in Fig. 6(a), the first mode is stable in the range $\omega_1\tau/(2\pi) < 0.34$ and un-

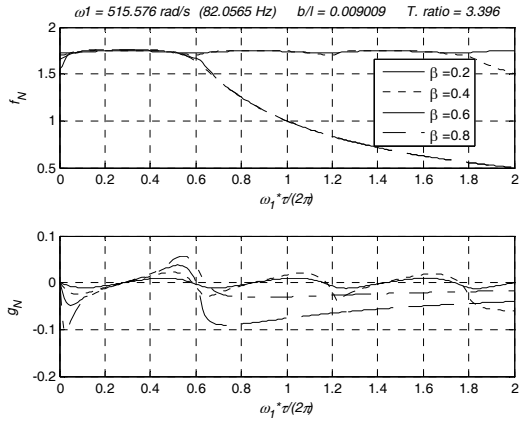

(a) 1st mode

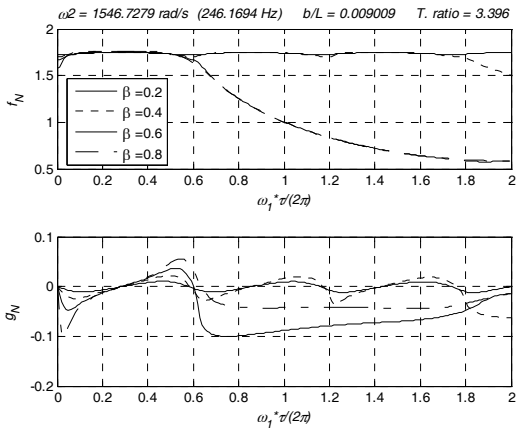

(b) 2nd mode

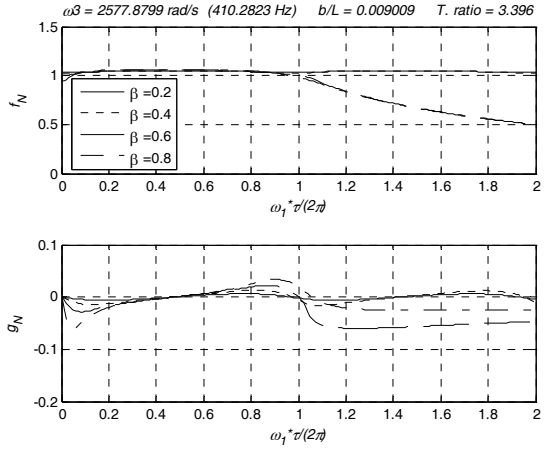

(c) 3rd mode

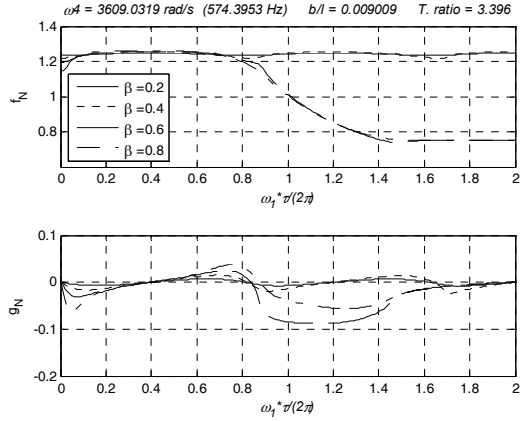

(d) 4th mode

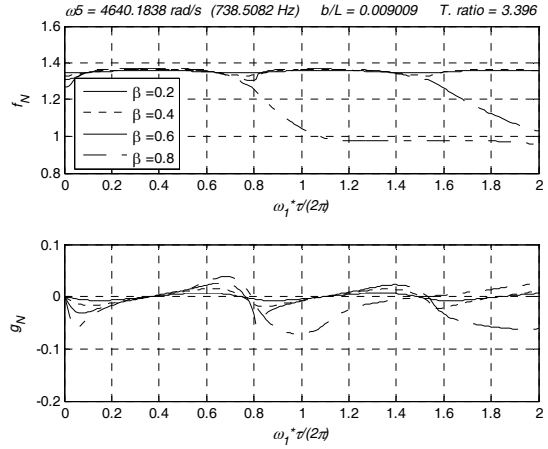

(e) 5th mode

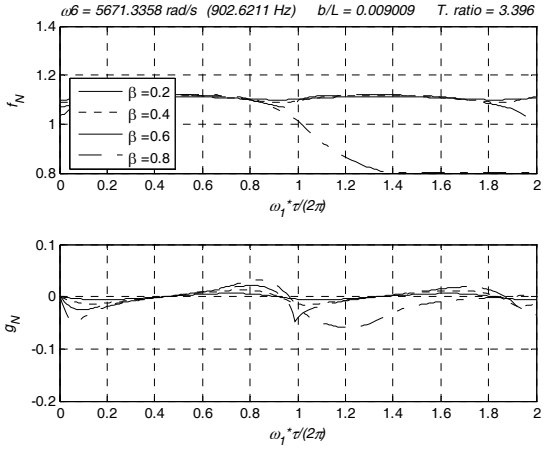

(f) 6th mode

Fig. 6. Variation of instability frequency and growth rate with τ for the root of Eq. (37) near the first ten undamped frequencies.

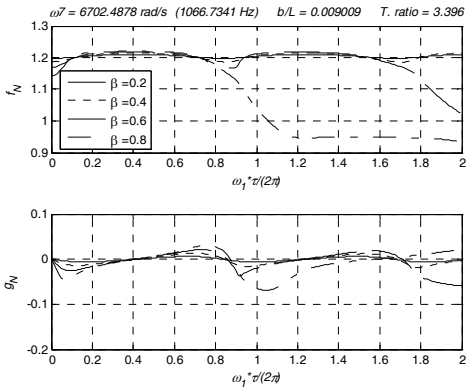

(g) 7th mode

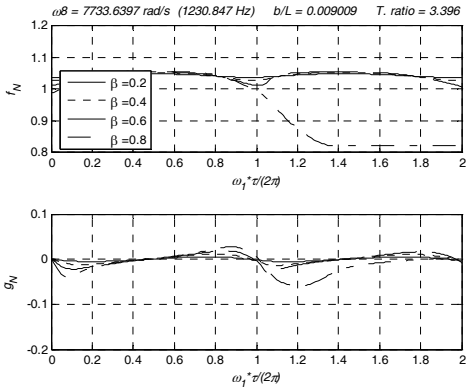

(h) 8th mode

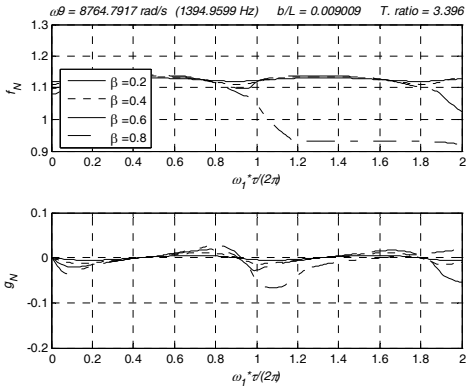

(i) 9th mode

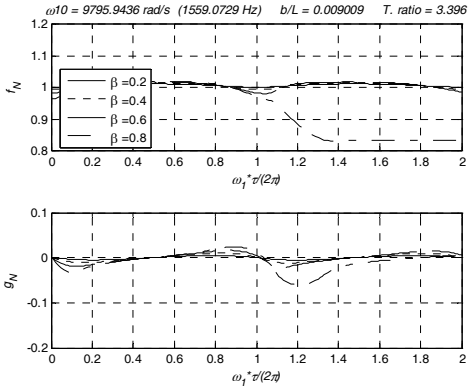

(j) 10th mode

Fig. 6. (continued).

Table 1. Simulation parameters of a case studied [4].

Parameter	Value	
	Upstream of flame	Downstream of flame
Section diameter, *m*	0.13335	0.13335
Section length,[1)] *m*	0.01270	1.39700
Temperature, *K*	553.3	1811.1
Pressure, *MPa*	2.020	2.020
Density, *kg/ m*^{3}	13.21	3.89
Ratio of specific heats	1.4	1.3
Mol. wt., *kg/kg-mole*	29	29
Sonic vel., *m/s*	462.7	821.6
Mean flow vel., *m/s*	7.64	25.93
Mach no.	0.01651	0.03156
Mass flow rate, *kg/s*	1.409	1.409

[1)] This parameter means *b* or (*l-b)* in Fig. 1 for upstream of flame and downstream of flame, respectively.

Table 2. Predicted combustion instability with traditional method for $\beta = 0.2$ shown in Fig. 6.

$\omega_1\tau^*/(2\pi) = \tau^*/T_1$	$f_N{}^*$	ω^*, Hz	A stable case (g_N<0)		An unstable case (g_N>0)	
			$\omega_1\tau/(2\pi)$	τ, ms	$\omega_1\tau/(2\pi)$	τ, ms
0.29	1.75	143.2	0.15	1.83	0.5	6.09
0.29	1.75	429.8	0.1	0.41	0.5	2.03
0.48	1.05	429.8	-	-	-	-
0.40	1.25	716.4	0.1	0.17	0.7	1.22
0.37	1.36	1003.2	0.1	0.14	0.7	0.95
0.45	1.11	1003.1	-	-	-	-
0.41	1.21	1290.1	-	-	-	-
0.48	1.05	1290.0	0.1	0.08	0.85	0.69
0.44	1.13	1578.2	-	-	-	-
0.49	1.01	1578.0	0.1	0.06	0.9	0.58

stable in the range $0.34 < \omega_1\tau/(2\pi) < 0.56$ at which g_N changes from a negative to a positive value. $f_N{}^*$ in the second column is the value of f_N at this transition point as shown in the figure. ω^* in the third column is the frequency that is obtained as $\omega^* = f_N{}^* \times \omega_N$ where

ω_N is the resonance frequency without the combustion. The next two columns show values of $\omega_1\tau/(2\pi)$ and τ for the stable case, i.e., $g_N < 0$. The last two columns are for the unstable cases.

Once the combustion process is represented by a control system, well-established tools such as the Nyquist plot, Bode plot or root-locus method can be applied. For example, the Nyquist plot provides qualitative information as to the degree of stability in addition to determining the absolute stability. If the system is stable, the corresponding Nyquist curve does not encircle the (-1,0) point. If the system is marginally stable, the curve passes through the point. If the system is unstable, the plot encircles the point. For a stable system, the closer the Nyquist curve approaches the (-1,0) point, the less stable the system is [13].

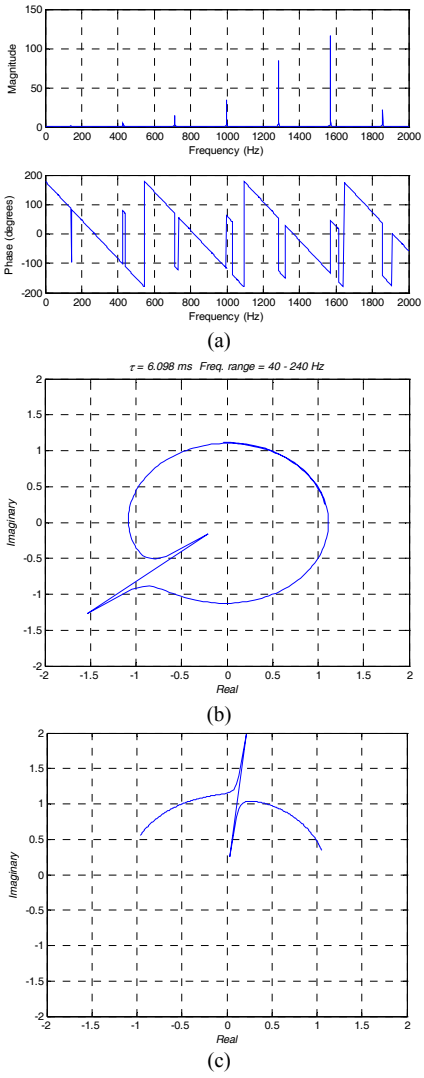

Fig. 7. The open loop transfer function K of a model combustion system studied: (a) Bode plot, (b) Nyquist plot of an unstable case at the 1st mode, and (c) Nyquist plot of a stable case at the 1st mode.

Fig. 7 shows the Bode and Nyqusit plots obtained for the case we study. The first one is the Bode plot of the open loop transfer function, which can provide the resonance frequencies of the model combustion system. Peak amplitudes in Fig. 7(a) correspond to the resonance frequencies of the system, which are listed in Table 3. As seen in the table, predicted resonance frequencies with this method agree well with those with the traditional system resonance frequency approach.

Next, Nyquist plots are used to see whether the system becomes stable or not at the given conditions. Fig. 7(b) is a Nyquist plot of the 1st mode ($\omega = 143.24$ *Hz* and $\tau = 6.09$ *ms*) which encircles (-1, 0) point, implying that the system is unstable. The case in Fig. 7(c) does not encircle the (-1, 0) point, and therefore is stable. Table 3 compares six resonance frequencies, which shows the equivalence of the methods.

6. Conclusions

A new method to study stability of combustors was developed in this work based on the transfer matrix method and a side-branch description of the system. The new approach enables to model the heat source as the input to the system; therefore enables modeling the system as a closed-loop feedback control system. The result from the model developed by the approach is compared with results from two existing methods.

The feed-back control system enables exploiting all the advantages of the classic control theories. Because of these advantages, the approach is very well suited

Table 3. Comparison of resonant frequencies with the two methods.

No.	ω, *Hz*		
	w/ traditional method	w/ feedback control concept	Difference (%)
1	143	142	1 (0.70)
2	430	428	2 (0.47)
3	716	713	3 (0.42)
4	1003	998	5 (0.50)
5	1290	1284	6 (0.47)
6	1578	1570	8 (0.51)

to design analysis of the combustion system.

The approach developed in this work can be further generalized for more accurate system analysis. The following generalizations of the approach are being considered in the future plan of the authors.

- Use more general heat source models.
- Include the effect of mean flow velocity.
- Apply the method to realistic combustion systems.
- Develop the system model with a 3-D description.

The first three will be straightforward. Although the last will require significant effort, the necessary techniques are well established [11, 14].

Acknowledgment

This work was supported by the New & Renewable Energy Center / Korea Energy Management Corporation through the project entitled "Design and Construction of 300 MW Class IGCC Demonstration Plant in Korea" funded by the Korean Ministry of Knowledge Economy.

Nomenclature

A,B,C,D	:	Four pole parameters
b	:	Length of a section in combustor
c	:	Speed of sound
f	:	Normalized frequency
g	:	Normalized growth rate
H	:	Transfer function
h_w	:	Heat source strength
j	:	Imaginary number $j^2 = -1$
k	:	Wave number
K	:	Open loop transfer function
l	:	Length of combustor
L	:	General length
$\dot{m}$	:	Mass flow rate
p	:	Acoustic pressure
P	:	Harmonic amplitude of p
q	:	The rate of heat release per area
Q	:	Harmonic amplitude of q
s	:	Cross-sectional area of section
t	:	Time
T	:	Period
u	:	Particle velocity
U	:	Harmonic amplitude of u
$\dot{W}$	:	Harmonic amplitude of $\dot{m}$
x	:	Spatial coordinate
Z	:	Impedance

Greek symbol

β	:	Nondimensional heat input parameter
γ	:	The ratio of specific heats
δ	:	Dirac delta function
η	:	Mode participation factor
ρ	:	Density
τ	:	Time delay
Ψ	:	Natural mode
ω	:	Angular frequency;

Subscript

i, m	:	Index
n, N	:	Undamped mode number, e.g., ω_n is natural frequency of the nth mode
s	:	Source
b	:	Indicates side branch
e	:	Indicates end

Superscript

-	:	Upstream
+	:	Downstream
*	:	The 1st stable-to-unstable transition condition

References

[1] L. Crocco, Aspects of combustion instabilities in liquid propellant rocket motors, 1. Fundamentals – low frequency instability with monopropellants, *Journal of the American Rocket Society,* 21 (6) (1951) 163-178.

[2] F. E. C. Culick, Combustion instabilities in liquid-fueled propulsion systems - An overview, AGARD Conference Proceedings, No. 450 (1989).

[3] P. E. Dowling and S. R. Stow, Acoustic analysis of gas turbine combustors, *Journal of Propulsion and Power*, 19 (5) (2003) 751-764.

[4] G. A. Richards, D. L. Straub and E. H. Robey, Passive control of combustion dynamics in stationary gas turbines, *Journal of Propulsion and Power*, 19 (5) (2003) 795-810.

[5] M. L. Munjal, *Acoustics of Ducts and Mufflers*, Wiley, New York, USA (1987) 121-130.

[6] J. Kim and W. Soedel, Analysis of gas pulsations in multiply connected three dimensional acoustic cavity with special attention to natural mode or wave cancellation effects, *Journal of Sound and Vibra-*

tions, 131 (1) (1989) 103-114.

[7] J. Kim and W. Soedel, General formulation of four pole parameters for three dimensional cavities utilizing modal expansion with special attention to the annular cylinder, *Journal of Sound and Vibrations*, 129 (2) (1989) 237-254.

[8] J. Kim and W. Soedel, Development of general procedure to formulate four pole parameters by modal expansion and its application to three dimensional cavities, *ASME Trans. Journal of Vibration and Acoustics*, 112 (1990) 452-459.

[9] J. E. Portillo, J. C. Sisco, M. J. Corless, V. Sankaran and W. E. Anderson, Generalized combustion instability model," *Proc. of 42nd AIAA/ASME/SAE/ASEE Joint Propulsion Conference & Exhibit*, Sacramento, CA, USA (2006).

[10] P. E. Doak, Analysis of internally generated sound in continuous materials: (i) inhomogeneous acoustic wave equations, *Journal of Sound and Vibration,* 2 (1965) 53-73.

[11] P. Kadam and J. Kim, Experimental formulation of four poles of three-dimensional cavities, *Journal of Sound and Vibration*, 307 (2007) 578-590.

[12] B. H. Schuermans and W. Polifke, Modeling transfer matrices of premix flames and comparison with experimental results, American Society of Mechanical Engineers, Paper 99-GT-132 (1999).

[13] C. L. Phillips and R. D. Harbor, *Feedback Control Systems*, 4th ed., Prentice-Hall, Upper Saddle River, NJ, USA (2000).

[14] W. Zhou, J. Kim and W. Soedel, Simulation of the cylinder process of refrigeration compressors by a numerical integration in the frequency and time combined domains with a special attention to a new iteration scheme, *ASME Trans. Journal of Mechanical Design*, 123 (2001) 282-288.

Dong Jin Cha received his B.S. and M.S. degrees from Hanyang University in Seoul, Korea, in 1981 and 1983, respectively. He then received his Ph.D. in ME from the University of Illinois at Chicago in 1992, and worked at the US DOE NETL for the next three years as a National Research Council (NRC) Associate. Dr. Cha is currently a Professor at the Department of Building Services Engineering at Hanbat National University in Daejeon, Korea. His research interests include combustion instability of gas turbine for power generation and fluid flows in building services engineering.

Jay H. Kim received his BSME from Seoul National University in 1977, MSME from KAIST in 1979 and Ph.D. in ME from Purdue University in 1988. He has joined the Mechanical Engineering faculty of the University of Cincinnati in 1990, and is currently a Professor. Before joining the University of Cincinnati, he worked in industry for six years in Korea and US. His research interests have been in broad areas of acoustics, vibrations and applied mechanics with recent focuses on human/bio-acoustics and vibration, gas pulsations and elastic stability.

Yong-Jin Joo received his BSME and MSME from Sung Kyun Kwan University in Seoul, Korea, in 1990 and 1992, respectively. Mr. Joo is currently a Project Leader for IGCC Operation Technologies at KEPRI (Korea Electric Power Research Institute) which is the central R&D center of KEPCO (Korea Electric Power Corporation). His research interests include the development of operation and maintenance simulator for power plants including IGCC.